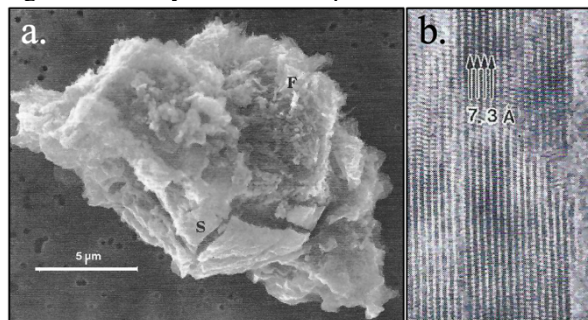


**GEMS ARE NOT PRECURSORS OF HYDRATED LAYER SILICATES IN IDPS OR “GEMS-LIKE” MATRICES IN CHONDRITES** J. P. Bradley<sup>1</sup>, H. A. Ishii<sup>1</sup>, D. J. Joswiak<sup>2</sup>, D. E. Brownlee<sup>2</sup>, K. Ohtaki<sup>1</sup>. <sup>1</sup>Hawai'i Institute of Geophysics and Planetology, University of Hawai'i at Manoa, 1680 East West Rd, Honolulu, HI 96822, USA. <sup>2</sup>Dept. of Astronomy, University of Washington, Seattle, WA 98195, USA.

**Introduction:** Approximately half of the interplanetary dust particles (IDPs) collected in the stratosphere are hydrated and contain layer silicates. Some Antarctic micrometeorites (AMMs) collected in snow and ice also contain layer silicates, and studies of their mineralogy and composition suggest that many have asteroid sources, consistent with observation and laboratory investigations showing that asteroids and Jupiter Family comets are major sources of dust at 1 AU [1-3]. Establishing the source of a hydrated IDP is more challenging because IDPs are much smaller than most AMMs, and therefore, their mineralogy is less diverse. As a result, only a few hydrated IDPs have been shown to be from asteroids [e.g., 4,5]. One example, IDP RB12A44 (Fig. 1), exhibits CM chondrite mineralogy [4]. Its layer silicates are compact, highly ordered and compositionally uniform, in contrast to the layer silicates in most hydrated IDPs that are poorly-ordered, compositionally heterogeneous on a ~50 nm scale and, relative to RB12A44, consistent with only limited compaction and aqueous alteration [6].

It is generally assumed that hydrated IDPs are from asteroids, but since localized aqueous alteration is certainly possible in nominally frozen bodies in the Kuiper belt (KB) [7], the limited degree of alteration in most hydrated IDPs raises the possibility that both they and GEMS-rich anhydrous IDPs are injected into the interplanetary medium in the KB. We are investigating the origin of layer silicates in hydrated IDPs by focusing on their anhydrous silicate precursors.



**Figure 1:** a) Secondary electron image of CM-type IDP RB12A44. F=fibrous; S=serpentine. b) Lattice-fringe image shows well-ordered serpentine. This IDP contains  $10^{11}$  cm<sup>-2</sup> implanted solar flare tracks.

**Results:** Data from three hydrated IDPs are shown in Figures 1-3. Layer silicate precursors are observed in all three. CM-type IDP RB12A44 (Fig. 1) is a fragment of a larger IDP that broke up on impact onto the collection flag. It contains abundant layer silicates (Mg- and Fe-rich serpentines), tochilinite, and minor

schreibersite, diopside, troilite, pentlandite, magnetite and possible sulfates. U230A34 (Fig. 2) consists of ~50% by volume perhaps-shock-fractured pyroxene (En<sub>95</sub>) and ~50% by volume compact smectite, Fe-rich silicate glass, and Fe-rich carbonates [6]. Sulfides and one or more enstatite platelets are embedded in the smectite. The Fe-rich silicate glass and enstatite are precursors of the layer silicates in this IDP (Fig. 2b). U2073B-8B (Fig. 3) is an ~8 μm diameter hydrated IDP that contains enstatite, forsterite, silicate glass and smectite. Enstatite (En<sub>92</sub>) is the dominant silicate mineral, and it is a precursor of the smectite (Fig. 3a). Overall, the smectite is poorly ordered although some regions display short-range order and ~1.4 nm lattice fringes (Fig. 3b). The smectite is Fe-rich (Mg/Fe = 0.2) and it also contains Na, Mg, Al, Ca and Fe (Fig. 3c,d).

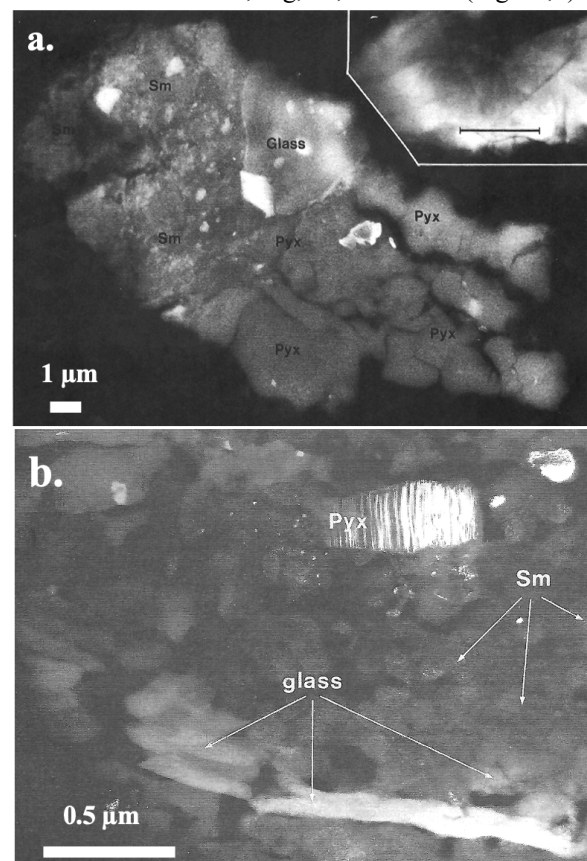


**Figure 2:** Hydrated IDP U230A34. a) Backscattered electron image shows (poorly-ordered) smectite (Sm), Fe-rich silicate glass and pyroxene (pyx) (~En<sub>98</sub>). The pyroxene contains solar flare tracks (inset, density ~ $8 \times 10^{10}$  cm<sup>-2</sup>). b) Darkfield image. Smectite precursors in this IDP are Fe-rich silicate glass and enstatite.

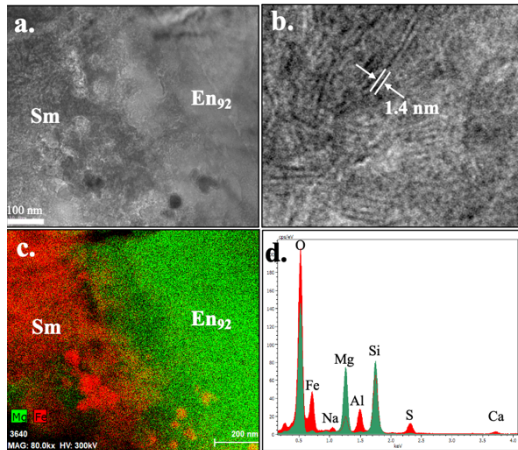


**Figure 3:** Hydrated IDP U2073B-8B a) Brightfield image of the interface between enstatite ( $En_{92}$ ) and Fe-rich smectite (Sm). b) Lattice-fringe image of the poorly ordered smectite. c) Energy-dispersive x-ray spectrum image of field-of-view in (a), Mg (green), Fe (red). d) EDX spectra (normalized to Si) of enstatite (green) and smectite (red).

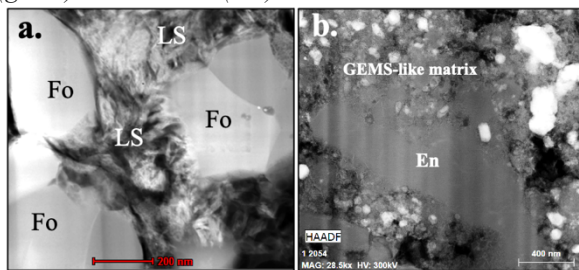


**Figure 4:** Darkfield images of chondrite matrices. a) Forsterite (Fo) altering to layer silicates (LS) in Paris CM chondrite. b) Enstatite altering to GEMS-like material in the (ungrouped) chondrite Acfer094 [8,9].

**Discussion:** Anhydrous silicates olivine, pyroxenes and silica rich glasses are typically minor constituents in most hydrated IDPs, and to date, we established that pyroxenes, especially enstatite, glasses and probably forsterite are precursors of layer silicates. These same silicates in hydrated matrices of carbonaceous chondrites are also layer silicate precursors (e.g., Fig. 4).

GEMS are conspicuously absent in hydrated chondritic materials we have examined. It is possible they were altered beyond recognition, but given the limited extent of alteration evident in most IDPs, some partially altered GEMS and especially their metal (kamacite) inclusions should survive. Rare “hybrid” IDPs and AMMs are an exception; they contain both GEMS and layer silicates but spatially separated and isolated within mineralogically distinct clasts [10,11]. Hybrid IDPs and AMMs are likely aggregates of fugitive particulates from parent bodies distributed over a range of heliocentric distances.

Materials that resemble GEMS but are not GEMS are found among chondrites and returned samples,

creating much interest in the relationship between *bona fide* GEMS in IDPs and GEMS-like matrix in chondrite matrices, and the possibility that GEMS are the precursors of GEMS-like matrix [e.g., 8,9,12]. We find that anhydrous silicates, but not GEMS, are precursors of GEMS-like matrix in chondrites (e.g., Fig. 4b).

Solar flare tracks may provide insight about the origin of layer silicates in hydrated IDPs arriving at 1 AU under the influence of Poynting Robertson (PR) drag [13]. IDP RB12A44 establishes that IDPs from asteroids have track densities as high as  $\sim 10^{11}$  cm $^{-2}$  [4]. Such high track densities are common among hydrated IDPs (e.g., Fig. 2a, inset). However, the range of track densities ( $10^9$  -  $10^{11}$  cm $^{-2}$ ) is the same among all classes of IDPs (and AMMs), including those of likely cometary origin, suggesting that PR drag alone cannot explain exposure ages. Particle trapping in planetary mean motion resonances, including the terrestrial planets, may increase exposure ages and solar flare track densities [14-16].

**Conclusions:** The precursors of layer silicates we have identified are crystalline silicates and silicate glasses but not GEMS. That GEMS are not precursors is highly significant; either they were never in the inner accretion disk, they were transient residents, or they were confined to the outer disk. Most likely they were never in the inner disk because the preserved mineralogy and isotopic compositions of GEMS establish that they formed in a cold (<50K) environment well beyond the influence of the young Sun, in the extreme outer nebula and interstellar medium [17, 18].

**Acknowledgments:** This research is supported by NASA grants 80NSSC19K0936 to HAI and 80NSSC20K0156 to DEB.

**References:** [1] Genge M.J. et al. (2020) *Planet. Space Sci.*, 187, 104900. [2] Dermott J.F. et al. (1994) *Science*, 369, 719-723. [3] Sandford S.A. and Bradley J.P. (1989) *Icarus*, 82, 146-166. [4] Bradley J.P. and Brownlee D.E. (1991) *Science*, 251, 489-496. [5] Keller L.P. et al. (1992) *GCA* 56, 1409-1412. [6] Bradley J.P. et al. (1990) *EPSL*, 101, 162-179. [7] de Burgh C. et al. (2004) *A&A*, 416, 791-798. [8] Villalon K.L. et al. (2021) *GCA*, 310, 346-362 [9] Ohtaki K. et al. (2021) *GCA*, 310, 320-345. [10] Noguchi T. et al. (2022) *MAPS*, 57, 2042-2062. [11] Joswiak D.J. et al. (2022) LPSC (this volume). [12] Ruggiu L.K. (2022) *GCA*, 336, 308-331. [13] Keller L.P. and Flynn G.J. (2021) *Nat. Astron.*, 6, 731-735. [14] Ruggiu L.K. (2022) *GCA*, 336, 308-331. [15] Grogan K. et al. (2001) *Icarus*, 52, 251-277 [16] Reach W.T. (2010) *Icarus*, 209, 848-850. [17] Christou A.A. et al. (2022) *MNRAS* 516, 1428-1441. [17] H. A. Ishii et al. (2018) *PNAS*, 115, 6608-13. [18] Bradley J.P. et al. (2022) *GCA*, 335, 323-338.